Liquids xenon and argon, dark matter detectors with background rejection

G. J. DAVIES

Imperial College of Technology and Medicine, High Energy Physics Group
Blackett Laboratory - Prince Consort Road, London SW7 2BZ, UK

(ricevuto il 12 Febbraio 1996; approvato il 4 Marzo 1997)

Summary. — The potential of liquids xenon and argon as dark matter targets is discussed emphasising the former. Significant discrimination of very small signals against beta/gamma backgrounds can be achieved in several ways; firstly via the collection of scintillation light alone in conjunction with a likelihood technique to fully exploit the digitised photon arrival times; secondly via the collection of both light and ionisation charge, either in a simple ionisation chamber or in the proportional scintillation mode. Published alpha and beta data are used to assess the discrimination.

PACS 07.07 – General equipment and techniques.

1. – Introduction

This paper examines the use of liquids xenon (LXe) and argon (LAr) in galactic dark matter experiments. Hence, one requires the detection of the small (< 50 keV) energy deposit of a nucleus recoiling from the elastic scatter of an incoming dark matter (DM) particle of mass 10–1000 GeV, moving with typical galactic velocities of 200–300 km s^{-1}. To search for DM particles at the rate predicted for the lightest super symmetric particle [1] (~ 0.01–1 events/d/kg depending upon its exact composition) requires discrimination against the beta/gamma background. Originally it was believed that energy thresholds obtainable with scintillators were not adequate for dark matter searches due to low light yields and difficulties of light collection combined with high background rates from photomultipliers. More careful examination of light collection and the increasing interest in higher mass WIMPs show scintillators to be of great potential [2]. Furthermore, they are suitable for scale-up to large target masses and may, as described below, offer significant background discrimination either via variations in the pulse shape of the scintillation light or via dual collection of light and ionisation charge [3].

The principal requirements of a dark matter scintillation detector are availability without radioactive contaminants and high light yields; these are met by LXe and LAr. 48% of naturally occurring Xe has odd mass number, hence nuclear spin, and is thus

sensitive to spin-dependent reactions. In addition, the high A offers good sensitivity to coherent interactions [1]. The overall time constant of the scintillation light emission in LXe is fast (< 50 ns with a component of ~ 3 ns), an advantage for detection by photomultipliers. However, the light is in the vacuum ultra-violet (VUV) with peak emission at ~ 175 nm—a significant disadvantage. As well as via the collection of light, detection can proceed through the collection of ionisation electrons, *i.e.* LXe can be used in ionisation chambers (*e.g.*, [4]).

Both the time spectrum of the scintillation light and the relative amount of charge produced depend on whether the source of ionisation is a densely ionising particle (such as a recoiling nucleus) or a lightly ionising particle (such as a beta or gamma ray from a radioactive contaminant). Thus, LXe offers good prospects for the discrimination of a dark matter signal from background; the relevant physical properties and the mechanisms of excitation, ionisation and scintillation are described in the following sections.

2. – Physical properties

Those physical properties of LXe most applicable to its use as a dark matter target are shown in table I.

3. – Scintillation and ionisation: the concept of discrimination

3˙1. *Scintillation mechanism.* – Charged particles in LXe lose energy by ionisation and atomic excitation [11]. Calculations [8] show that, for incident betas, the ratio of the initial number of excitations (N_{ext}) to the initial number of ionisations (N_i) is

$$N_{\text{ext}}/N_i \sim 0.06\,. \tag{1}$$

In excitation (also referred to as self-trapping), the electron remains bound to the hole as an exciton. Migration of excitons is stopped within picoseconds by the formation of

TABLE I. – *Physical properties of liquid xenon.*

Atomic mass	131
Density of liquid	3.06 g/cm^3
Boiling point at 1 atm.	160 K
Refractive index (at 175 nm)	1.603 [5]
Peak scintillation emission	175 ± 15 nm [5]
Attenuation length	40 cm [5]
Light yield	20–70 photons/keV [4-7] ([a])
Decay constant (min ionising)	
fast	$\tau_1 = 3$ ns [8]
slow	$\tau_2 = 27$ ns [8]
Recombination time (min ionising)	15 ns [9]
Fano-factor	0.041
W-value (eV/ion pair)	15.6 or 9.8 [9, 10] ([a])

(*a*) The different values reflect the variation between references.

the excited metastable excimer, Xe_2^*,

$$Xe^* + Xe \rightarrow Xe_2^* . \tag{2}$$

Alternatively, in ionisation, the electrons are ejected from the atom to which they were originally bound and are free to travel through the LXe [4]. However, the resulting holes are quickly localised by the formation of the Xe_2^* ion which has ~ 1 eV less energy than the separated Xe^+-Xe configuration [12]. The free electrons lose energy via the creation of further excitons, so increasing the calculated number of excitations, the production of further electron-hole pairs and finally through the emission of phonons. If the free electrons from an incident beta are not lost during thermalisation to the external electric field of an ionisation chamber, about 1/3 recombine with the localised Xe_2^* to form the excited metastable excimer state again,

$$Xe_2^+ + e^- \rightarrow Xe_2^* . \tag{3}$$

The lowest lying electronic energy levels of the excimer are responsible for the scintillation light, *viz.*, the singlet, $^1\Sigma_v^+$, and triplet $^3\Sigma_u^+$ [7]. With $\tau_1 \sim 3$ ns and $\tau_2 = (27 \pm 1)$ ns lifetimes, respectively [8], each emits a monochromatic VUV photon with $\lambda = (175 \pm 15)$ nm in decaying to the respulsive ground state which then flies apart emitting phonons:

$$Xe_2^* \rightarrow Xe_2 + \text{photon} \rightarrow 2\,Xe + \text{phonons} . \tag{4}$$

3˙2. *Pulse shape and light yield.* – A nuclear recoil (NR) from an incident DM particle will be heavily ionising and so produce a signal more akin to that of an alpha than that of a beta, indeed it is most likely that the NR will in fact be more heavily ionising than the alpha. The following results have been achieved with α and β sources of a few MeV.

For incident β, the scintillation light has three time components [13]: the above two exponential decays from the singlet and triplet states of the excimer formed from self-trapped excitons (26% of the light yield) and also that of the recombination luminescence (74% of the light yield) resulting from excimer decays following recombination of ions [8]. The latter process is delayed by the recombination time of about 15 ns [9] so that the overall photon time spectrum has an exponential form with a time constant of about 45 ns, although the non-exponential tail may extend to 2 μs [14].

Incident alpha particles, because of their lower velocity and greater charge, have a much higher linear energy transfer (dE/dX) than betas of the same energy. In fact, alphas produce about 2 electron-hole pairs per Å compared with 0.002 for betas [14]. Thus for incident alphas, the recombination time of ions is very short and so there is no time distinction between photons from excitation production ([1]) and from recombination of ions. Additionally, it has been found that the excimer singlet decay ($\tau_1 = 3$ ns) is considerably stronger than the triplet decay ($\tau_2 = 27$ ns). Let A_1 and A_2 be the amplitudes of the exponentials describing the singlet and triplet states. The ratio $A_1 : A_2$ has been found to be 7.5 by Kubota *et al.* [15] and Hitachi *et al.* [14]. This is

([1]) The thermalisation of the ionised electrons and the de-excitation of the excited excimer to its lowest-lying states occur within picoseconds.

very different to the case of incident betas where the measured ratio is about 0.8 [8], *i.e.*

$$\left(\frac{A_1}{A_2}\right)_\alpha = 7.5 \quad \text{and} \quad \left(\frac{A_1}{A_2}\right)_\beta = 0.8 . \tag{5}$$

For an incident alpha-particle the observed light intensity per ns seen at a time t is thus given by

$$L_\alpha(t) = A_{1\alpha} \exp[-(t/\tau_1)] + A_{2\alpha} \exp[-(t/\tau_2)] \tag{6}$$

and by

$$L_\beta(t) = A_{1\beta} \exp[-(t/\tau_1)] + A_{2\beta} \exp[-(t/\tau_2)] + F(t_r) \tag{7}$$

in the case of an incident beta. The term $F(\tau_r)$ is due to the non-exponential recombination process and when written in full is given in [8],

$$F(\tau_r) = f_1 \times \tau_r \times \int_0^{t'} \frac{(t/\tau_r)}{(\tau_r + t)^2}\, dt \times \exp[-(t/\tau_1)] + (1 - f_1) \times \tau_r \times \times \int_0^{t'} \frac{\exp[t/t_r]}{(t_r + t)^2}\, dt \times \exp[-(t/\tau_2)], \tag{8}$$

where f_1 is the fraction of excimers produced in the singlet state by recombination. The resulting $L_\beta(t)$ has a time profile (both calculated [8] and observed [16]) which is approximately exponential out to 100 ns, falling with an effective time constant, $\tau_\beta \sim 45$ ns, within this period.

Thus,

$$L_\beta(t) \sim A_\beta \exp[-(t/\tau_\beta)], \quad \text{where } A_\beta = 1/\tau_\beta \text{ such that } \int_0^\infty A_\beta\, dt = 1 . \tag{9}$$

The resulting pulse shapes are shown in fig. 1.

Significant light saturation ([2]) is not observed with LXe. If we define L/E as the light intensity per unit energy for a given incident particle, then experiments show that [14, 15]:

$$\left(\frac{L}{E}\right)_\alpha \Big/ \left(\frac{L}{E}\right)_\beta \sim 1.1 . \tag{10}$$

This is somewhat surprising until one recalls the faster recombination time for incident alphas; it would not be unreasonable to suppose that the faster the recombination, the

([2]) By saturation we mean the overall reduction in light yield, for a given energy deposited, for a heavily ionising particle in comparison to a lightly ionising particle. Quenching is the process by which the primary excitation is reduced due to interactions between the closely packed ionised and excited molecules which occur along the track of a heavily ionising particle [17].

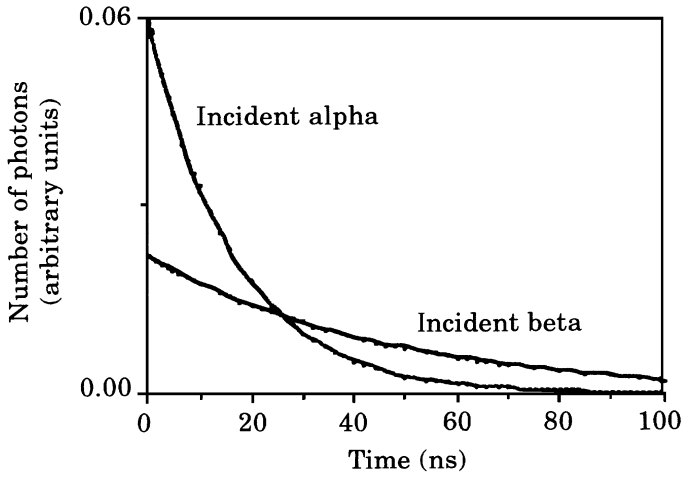

Fig. 1. – Schematic plot of light yield *vs.* time for LXe for alphas and betas of equal energy.

smaller the fraction of thermalised electrons and ions lost, *i.e.* one might expect

$$\left(\frac{\Lambda}{E}\right)_{\alpha} \Big/ \left(\frac{L}{E}\right)_{\beta} \leqslant 1/4 + (3/4 \times 3) \sim 2.5\,, \tag{11}$$

where the "1/4" results from the fact that 1/4 of the light emitted for an incident beta is due to self-trapping ([3]), and the factor of 3 from the fact that, for incident beta, only about 1/3 of them recombine. Hence, it is conjectured that quenching is taking place for an incident alpha, but the effect of this quenching is compensated for by the factor of $\leqslant 3$ gain in the number of recombinations and so the overall ratio of light yields for alphas and betas is as given by eq. (10). Hopefully, future work will clarify this important issue.

3˙3. *Charge collection.* – Similar considerations apply to LXe in an ionisation chamber. Typically, the energy resolution for a 0.57 MeV γ is $\sim 6\%$ at f.w.h.m. This is good but much worse than the 0.3% predicted from the low values of $W \leqslant 15.6$ eV and Fano-factor, $F = 0.04$ [18, 19]. For a long time this was attributed to impurities, but fluctuations in the recombination of the delta rays are now held to be responsible for the poorer resolution. The resolution does not saturate with increasing electric field [4]. Recently, Ypsilantis and Seguinot have suggested that the best energy resolution can be achieved by dual collection of both light and charge [10]. For incident alpha, owing to fast recombination, only $\sim 1/15$th of the electrons can escape recombination to be collected by an external electric field [20]. This paucity of electrons is confirmed in photo-ionisation experiments [21].

3˙4. *Figure of merit.* – The above properties of LXe suggest that heavily ionising particles can be distinguished from β/γ events down to very low energies via the ratio

([3]) One assumes that this light is unaffected by the change of incident particle.

$A_1 : A_2$, with the latter also being identified by their production of free electrons which can be collected in an ionisation chamber or via proportional scintillation. Such discrimination can be achieved either by detecting both the excitation and slow recombination light (A) or the excitation light alone and the electrons before they recombine (B). Let us consider each method in turn.

To assess the discrimination achievable with each, a figure of merit, FM, following the notation of Smith *et al.* [22], is introduced:

$$\text{FM} = \frac{(f_\text{b}^{1/2}(1-f_\text{b})^{1/2})}{(f_\text{n}-f_\text{b})}\ , \tag{12}$$

where f_b is the fraction of background events remaining when a fraction, f_n, of nuclear recoil events are detected. Thus the *greater* the *discrimination*, the *smaller* FM.

4. – No electric field applied to the LXe: method A

The easiest mehod of discrimination from the point of view of detector construction is a pure scintillation counter in which both the primary and secondary light are detected because the least stringent levels of liquid purity are required ([4]). One could consider simply comparing the number of photons detected within a short interval to those detected within a long interval to distinguish background from signal in a method analogous to conventional n-γ discrimination in neutron counters [24]. However, such a simple technique loses information.

Better discrimination can be achieved by accurately recording the arrival times of photons within a scintillation light pulse and using a likelihood ratio method to compare the probability that the photons were initiated by a nuclear recoil or a background beta. This requires the arrival time of each photon to be known to ~ 1 ns, which can be obtained with suitable photomultipliers and flash ADCs.

Although the curves in fig. 1 have been produced by recording the arrival times of thousands of photons from the LXe, the functions $L(t)$ still have meaning in the context of a single photon. Here, they represent the *probability* or *likelihood* for a particular photon to arrive within that ns time interval. The product of the probabilities (or sum of the log of the probabilities) for each photon arrival time within a pulse can be taken to form the likelihood function, LF, that the pulse was initiated by a beta or alpha particle. Indeed the ratio (R) of the likelihood functions may be taken and its distribution with the number of photon arrival times and initiating particle studied.

To assess the level of discrimination possible at low photon numbers, a simulated analysis of the arrival times of detected photons was carried out. A fixed number, N_γ, of detected scintillation photons is selected at random from $L_\beta(t)$. The likelihood function, $\text{LF}_\beta = \mathbf{P}_N L_\beta(t)$, for those N_γ photons to have come from a beta is calculated along with the corresponding likelihood function, $\text{LF}_\alpha = \mathbf{P}_N L_\alpha(t)$, for the N_γ as if they had come from an incident alpha. The ratio, R, of these two likelihood functions is then taken (here $R = \text{LF}_\alpha/\text{LF}_\beta$). This process is repeated many times for the same value of N_γ to produce a distribution of R for betas for this value of N_γ. The value of N_γ is then varied and a distribution of R produced for the new value of N_γ. The procedure is repeated for

([4]) It is expected that a detector involving the drifting/collection of charge requires 10–100 times lower impurity levels than one based upon the collection of light alone [23].

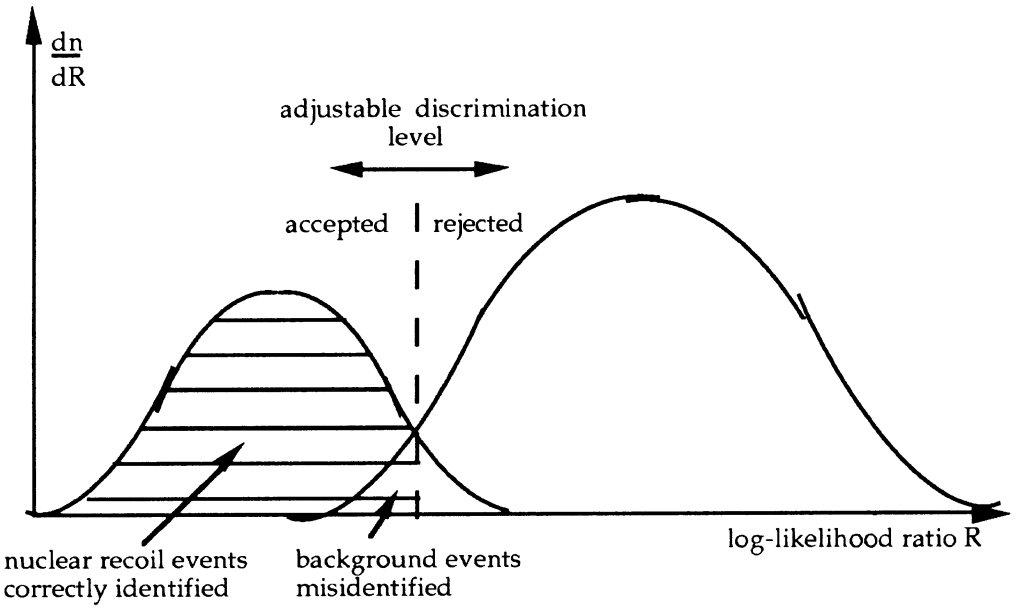

Fig. 2. – Illustrative log-likelihood ratio, ln R.

photons selected at random from $L_\alpha(t)$ to allow a distribution of R as a function of N_γ to be built up for alpha events.

The overlap in the two R distributions for the same N_γ is studied (for convenience ln R is usually plotted); they will by definition overlap at $R = 1$ (ln $R = 0$). One can choose any discrimination value, R_d, to reject a given percentage of background events. However, as the fraction, f_b, of beta events rejected, and hence the purity is increased, the fraction, f_n, of nuclear recoil events correctly identified decreases. Thus, there is a trade-off between signal detection efficiency and background rejection. This is illustrated schematically in fig. 2.

The single photoelectron (s.p.e.) pulse shape will not be a delta-function and its finite width causes pulses to overlap, so that it is impossible to tell from the overall PMT pulse shape how many photons have arrived or when. Thus, it was decided to read the pulse shape each ns and treat this pulse height as an effective number of photon arrival times. The single photoelectron (s.p.e.) pulse shape as recorded by a 2-inch fast plano-concave quartz tube (EMI QB9229 with modified dynode) of f.w.h.m. 3 ns and base width 6 ns was fed into the parent distribution function. Treating the s.p.e. pulse shape in this manner increases the magnitude of the likelihood functions (*i.e.* affects the x-axis) but does not significantly affect the overlap. Widening the s.p.e. pulse shape to a full base width of 9 ns had very little effect. Figure 3 shows Monte Carlo results, with the observed s.p.e. pulse shape included.

The percentage of alphas correctly identified for a background rejection of 95% ($f_b = 0.05$) is shown as the uppermost curve in fig. 4. Even with increased levels of background rejection, the two broken curves, the percentage of alphas identified is still high. For 95% background rejection the figure of merit varies from 0.29 to 0.24

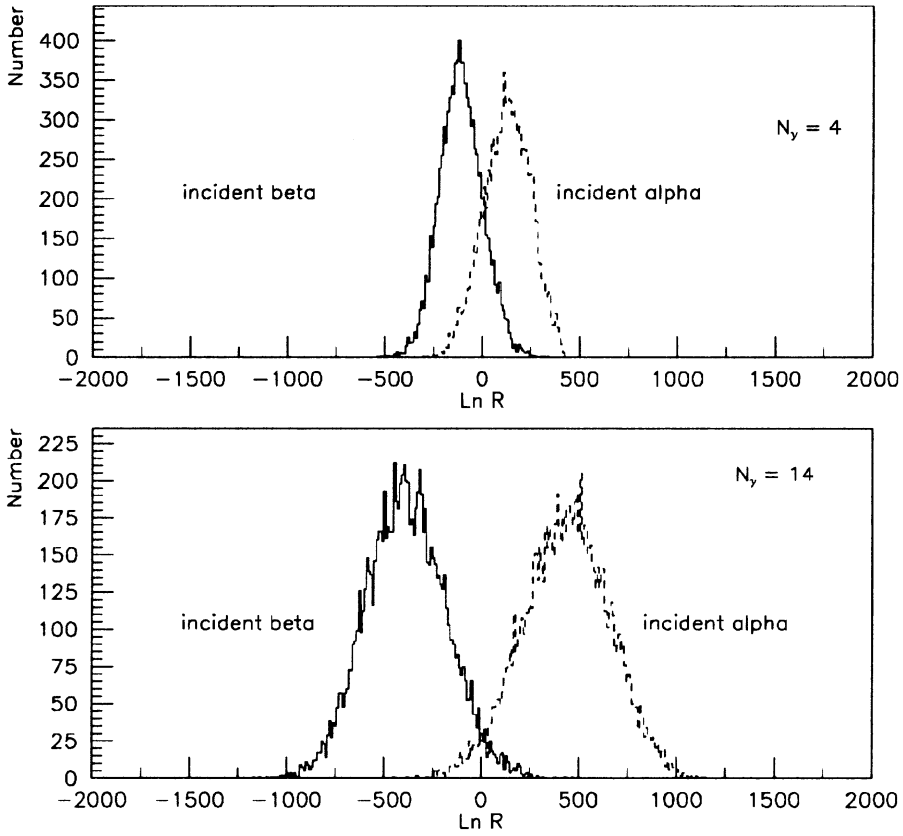

Fig. 3. – Likelihood with PMT s.p.e. pulse shape included.

as N_γ varies from 6 to 12; for a background rejection of 99.95 the respective values are 0.11 and 0.03.

As well as genuine scintillation signals, spurious signals will result from noise in the PMTs. The effect of this noise is twofold. Firstly, it will degrade the discrimination between alpha and beta pulses. To assess this random Poissonian noise pulses were included in the parent distribution functions (and hence the N_γ) as for the single photoelectron pulse shape. The effect of noise can be seen as the lower of the two solid curves: an extremely conservative rate of 1 kHz was taken. There is slight degradation in discrimination, which is little worsened if the noise rate is increased.

Secondly, the noise pulses could possibly mimic an alpha event. Thus the effect of replacing the N_γ arrival times from the alpha parent distribution function with N_γ times from a random noise distribution was also studied. The overall rate of false identifications will be given by the product of the percentage of noise events identified as alpha events and the probability of producing N_γ random times within that time period, t. The daily rate is given in table II for the two cases of PMTs in coincidence or summed. (Values of 1 kHz for the noise rate per tube and $t = 30$ ns were used.)

Hence an operational threshold can be set at $N_\gamma \geqslant 3$ to limit the number of false identifications per day to tolerable levels whilst still allowing significant levels of

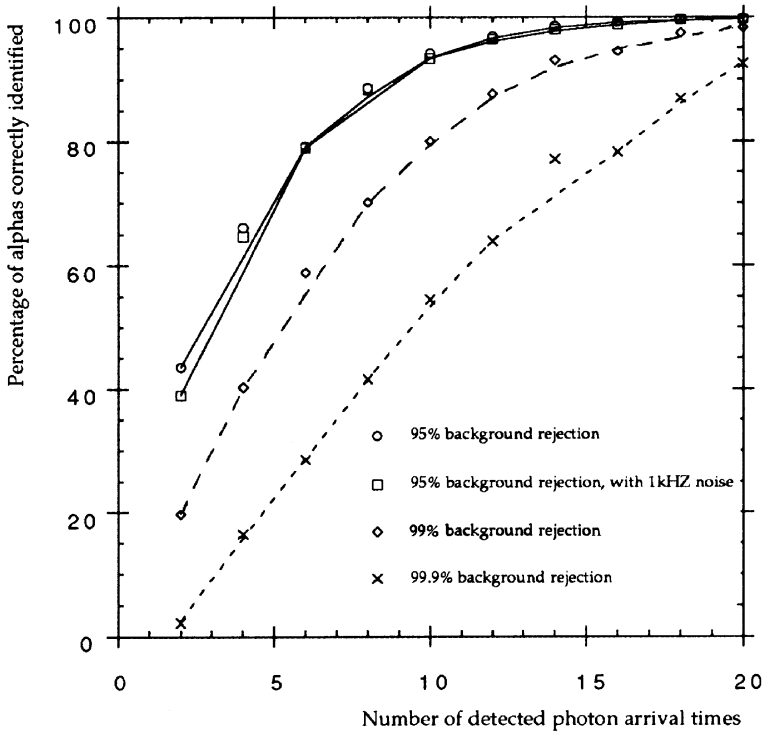

Fig. 4. – Percentage of alphas correctly identified as functions of background rejection and number of detected photon arrival times.

TABLE II. – *Rate of false signals from random noise.*

Number of photon arrival times within time t (30 ns)	Rate/day of falsely identified noise events for PMT outputs	
	summed	in coincidence
2	4500	2200
3	0.34	0.086
4	2.5×10^{-5}	3.1×10^{-6}

discrimination. With a light collection of 25% and a PMT photocathode efficiency of 20% (≡ an overall light detection of 5%), this threshold corresponds to just 2 keV.

The effects of the quantised digitisation and the time spread of photons along the light guide were found to be negligible. The distinctive time structure of nuclear decays within the PMT and afterpulses means that they can be rejected without any significant loss of genuine signal events.

5. – Electric field applied to the LXe: method B

If the LXe detector incorporates charge collection, improved discrimination is achievable. Consider the following, where the energy appearing as scintillation light is signified by E_s and that appearing as ionisation by E_i.

a) For incident betas, $< 10\%$ of the energy produces direct scintillation (via excitation) whilst $> 90\%$ produces ionisation with a proportion of this appearing as light. The application of the electric field will suppress recombination and a high proportion ($> 80\%$) of the ionisation can be collected. Thus the ratio of the energy depositions for a beta is

$$(RS_{\text{energy}})_\beta = (E_s/E_i)_\beta < 1 . \tag{13}$$

b) For incident alphas, the ionisation that can be collected for a given electric field is smaller ($\sim 1/15$th) as mentioned in subsect. **3**·3, even at maximum field strength. The remaining 94% of the energy will appear as light, with a scintillation efficiency of $\sim 75\%$ from [3]. Thus, the ratio of the energy depositions for an alpha is

$$(RS_{\text{energy}})_\alpha = (E_s/E_i)_\alpha \sim 10 . \tag{14}$$

Hence, the ratio of the ratios of energy depositions is

$$RRS_{\text{energy}} = \frac{(E_s/E_i)_\alpha}{(E_s/E_i)_\beta} > 10 . \tag{15}$$

The discrimination available with this technique can be studied by using a Monte Carlo based on the data of subsects. **3**·2 and **3**·3 to give the light and charge signals. In particular, recall that i) for an incident beta, $\sim 1/3$ of e^-/ion pairs recombine to give light but the application of an electric field can reduce the total light yield by 75%, but allows only 90% of the charge to be collected; ii) for an incident alpha, only $\sim 1/15$th e^-/ion pairs escape recombination to be collectable by an E field.

Defining

$$RS_{\text{signal}} = \frac{\text{size of the light signal}}{\text{size of the charge signal}} , \tag{16}$$

then the overlap in $(RS_{\text{signal}})_\alpha$ and $(RS_{\text{signal}})_\beta$ can be studied as a function of the energy deposited in the LXe and the resolution of the light and charge detectors. For the energy range under question ($\sim$ 5–20 keV) conservative Gaussian resolutions of 30–50% for both light and charge collection were considered as there is limited experimental data [23, 25]. A light yield of 30 photons/keV and a charge yield of 64 e^-/ion pairs/keV were used. Hard thresholds of 2 photoelectrons and 50 electron noise equivalent were set below which events were classed as lost (no Poisson correction was applied close to threshold).

Figure 5 shows the distribution of the log of the ratio of eq. (15) for those alphas and betas detected for observed energies of 10 and 20 keV for resolutions of 30 and 50%, for the same number of incident alphas and betas.

Clearly there is significant discrimination. Indeed at both energies, for a simple cut at $\ln(RS_{\text{signal}}) \sim -3$, over 99.5% of the detected alphas are correctly identified whilst

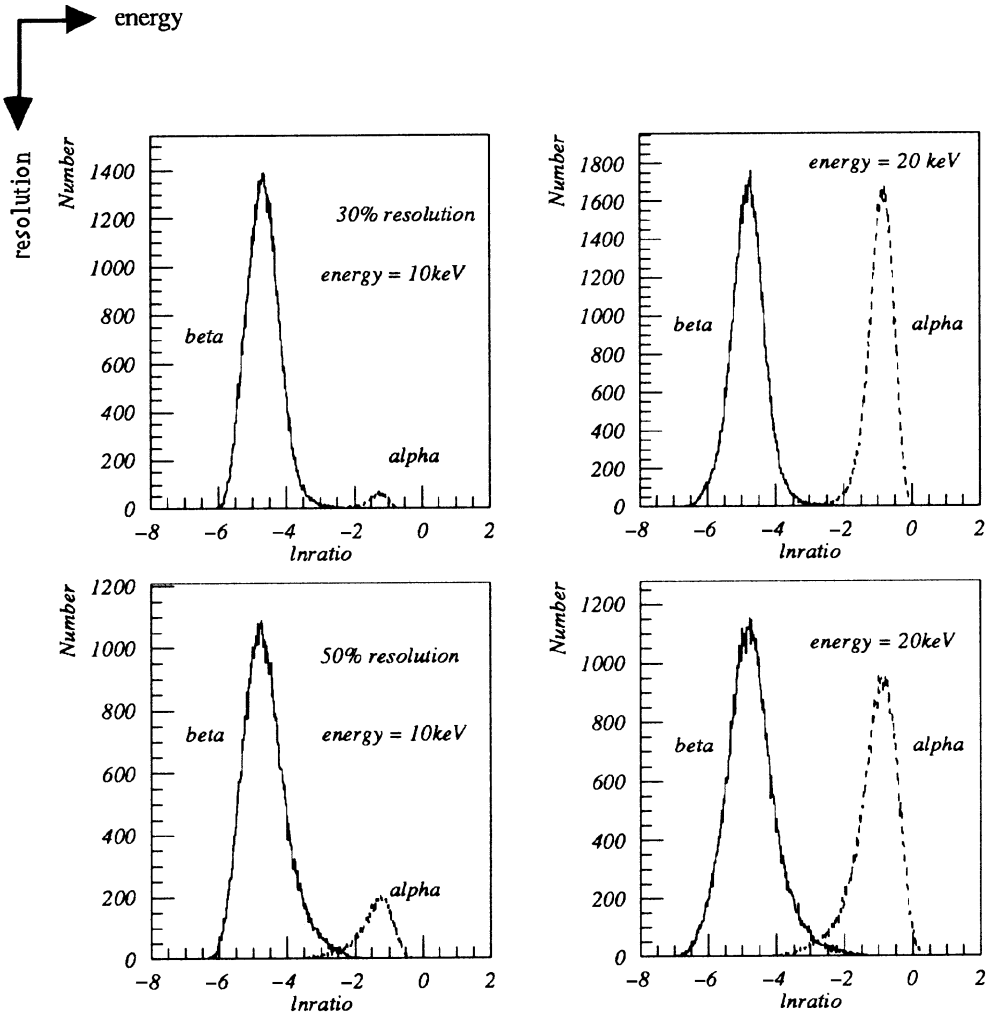

Fig. 5. – Overlap in $\ln(RS_{\text{signal}})$ for 30% and 50% resolutions.

the background contamination is $\leqslant 1\%$. However, such figures are misleading as light and charge signals are frequently not simultaneously above threshold. Figure 6 shows the fraction of light and charge signals which are brought below threshold by the statistical fluctuations for an energy resolution of 40% for incident beta and alpha; the alpha charge pulse is most affected.

The alpha and beta detection efficiencies could be calibrated across the desired energy band. However, a far more satisfactory solution for such a large correction is the amplification of the charge signal. This can be achieved via proportional scintillation—using the drifted electrons to cause the xenon to give a second delayed light pulse in a region of higher electric field—or directly via the use of sharp anode tips which greatly increase the local electric field. Each will be considered in turn.

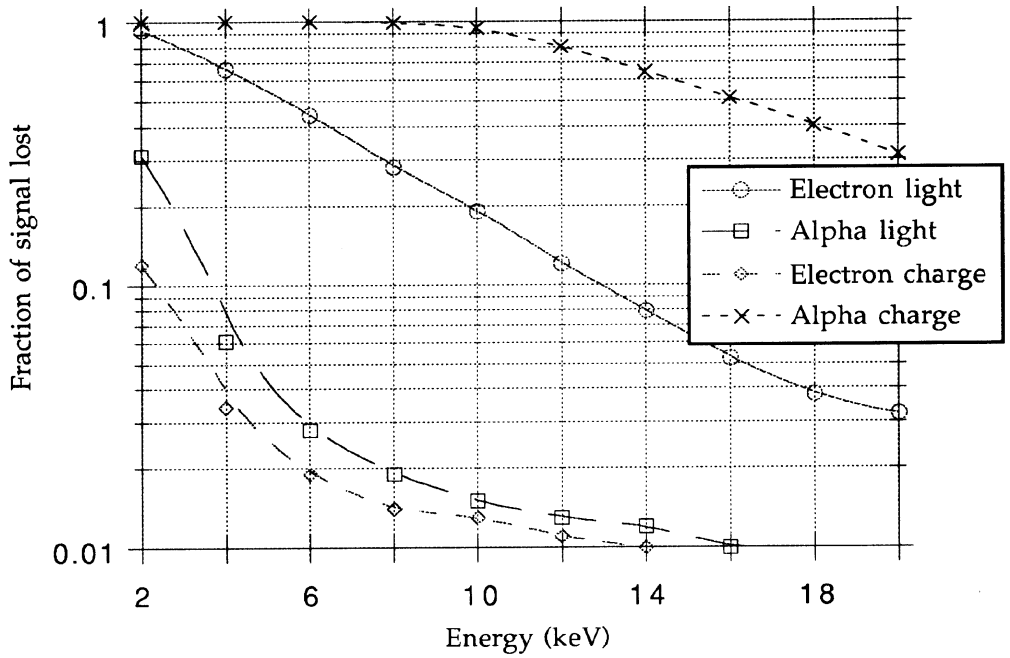

Fig. 6. – Fraction of light and charge signals below threshold for 40% resolution.

6. – Amplification of recombination light—proportional scintillation

The development of a practical proportional scintillation counter in the liquid phase is complex; consequently, several groups have initially chosen to study the unamplified scintillation light from LXe alone. However encouraging results have recently been reported at CERN [26] and a joint UK-UCLA proportional scintillation proposal has now been submitted [27]. The different scintillation pulses as observed by the CERN based group for incident alpha and beta are shown in fig. 7, taken from [26]. S1 corresponds to the direct scintillation light pulse and S2 to the delayed light pulse due to the drifted electrons.

Thus an alpha is identified by an S1/S2 ratio $\gg 1$ and a beta by an S1/S2 ratio < 1. In the following, the discrimination achievable via the measurement of S1 and S2 will be discussed.

Whilst the CERN group report that 122 keV gamma rays only give a single pulse (S1 missing) 1% of the time, they do not consider the overlap in the pulse height ratios for incident particles of more equal and lower energy. It is possible to apply the same Monte Carlo as used in sect. **5** to consider this problem. A multiplication factor of 40 photons per beta was used [28]. The CERN group observed the same resolution for both S1 and S2 (40% at 122 keV) and we took this as including the fluctuation in the multiplication process. As a consequence, throughout the proportional scintillation simulation a resolution of 40% was taken in all cases except those for which the error given by $1/\sqrt{N}$, where N is the number of photons detected by the photomultiplier,

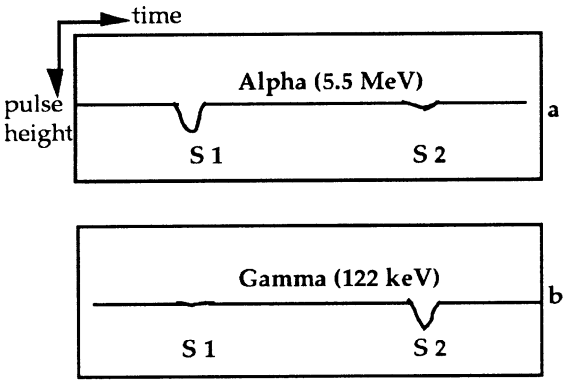

Fig. 7. – Scintillation signals from 3 μm wires for an anode to cathode voltage of 3.0 kV. (S1 is the direct light pulse and S2 the delayed light pulse, taken from [26].)

was greater ([5]). At 122 keV the Monte Carlo gave, for overall light collections of 5–8% and thresholds of 2–4 photoelectrons, a single pulse about 1% of the time, in agreement with the CERN result.

Even at low energies there is still very good discrimination, as can be seen from fig. 8, which again considers the same number of incident alphas and betas.

Note, in comparison to fig. 5, it is now possible to form ratios at 4 keV. For both incident beta and alpha less than 1% of events fail to give a secondary light pulse and thus the number of events which allow a ratio to be formed is governed by the fraction having detectable primary light (recall fig. 6). If we treat an event which gives a single pulse as unidentifiable, the circular points in fig. 9 give the overall signal identification and background misidentification at a resolution of 40% for a $\ln(S_1/S_1)$ cut at -3.5. The figure of merit for an observed energy of 4 keV ($\approx$ 6 detected photons) is 1.78 and for an observed energy of 14 keV ($\sim$ equivalent to 20 detected photons) is 0.33.

These numbers can be improved. Associating the charge pulse on the anode grid with a single light pulse identifies it as S2. Furthermore, for events with S1 below threshold figs. 6 and 7 show that betas produce larger S2 pulses than alphas. To quantify this, random events from a uniform beta energy distribution and from the expected exponential DM curve for the alpha were generated in the desired range (0–20 keV). For "S2 only" events, a cut was placed on the size of the S2 signal such that $\sim$ 75% of the alpha events fell below this and hence were accepted. Typically about 10% of the beta "S2 only" events fell below this cut and so were misidentified. The square points in fig. 9 show the improved discrimination; the figure of merit improves to 0.12 for energies above 4 keV. A small percentage of events ($< 1\%$) give only an S1 pulse; as these are more likely to be alphas, they were classed as such ([6]).

([5]) The only published energy resolution at low energies is $\sigma/E = 0.0495 + 1.63/\sqrt{E}$ (keV) [25], which gives 20% at 122 keV. Using this resolution little affected the discrimination observed.

([6]) Alternatively as the number of "S1 only" events is smaller than in sect. **5** due to the amplification of the ionisation electrons, all single pulse events can be ignored and the final event rate corrected for, as discussed in sect. **5**.

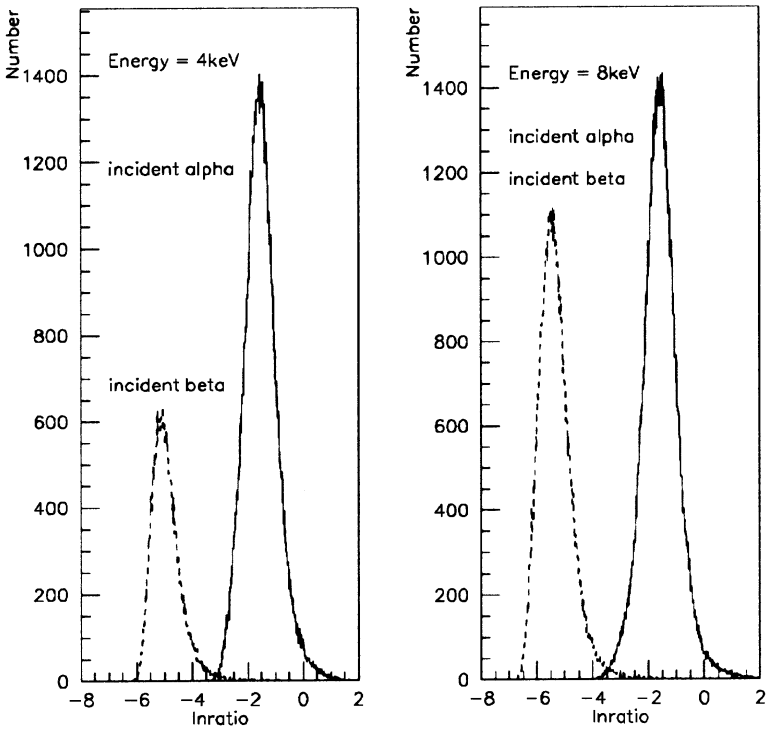

Fig. 8. – Overlap in proportional scintillation $\ln(S_1/S_1)$ at 4 and 8 keV for a resolution of 40%.

Whereas improved figures of merit were possible in sect. **4** by looking at greater levels of background rejection, the fact that ratios of actual signal sizes are being taken here, for properties which each have variation, leads to greater tails on the overlap plots. Hence it is not possible to set a higher background rejection level without significantly reducing the fraction of signal collected.

A further refinement would be to record the arrival times of the prompt photons and perform a likelihood ratio test on the $\sim 1\%$ of events for which only S1 is seen. For betas in the range 4–20 keV the mean signal size varies from 3 to 8 photoelectrons, whilst for alphas it varies from 6 to 30 photoelectrons. Although the power of such a likelihood test would be less in this case as there is no recombination light, initial studies indicate that, in rejecting 95% of the betas, then typically 80–30% of the signal will also be rejected as the number of photon arrival times is varied from 2 to 20. However, a more significant use of the likelihood technique would be to reject random coincidences between light and charge pulses originating from noise.

The experimental value of $(A_1/A_2)_\beta \sim 0.18$ in the presence of an electric field was taken from [8]. This corresponding ratio for alphas can only be inferred approximately from the possible explanations for the experimentally measured ratio without an electric field. A conservative value of 5 was taken for $(A_1/A_2)_\alpha$ in the presence of an applied E field.

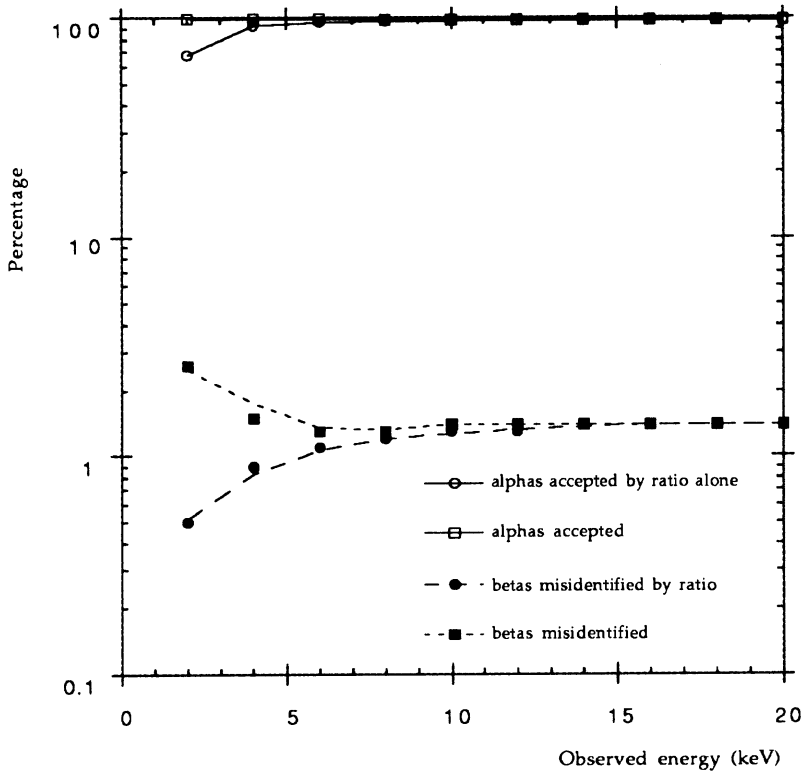

Fig. 9. – Percentage of events identified and misidentified.

7. – Direct amplification of charge—anode tips

Recently Bressi *et al.* [29] have shown that gains of 100 are possible by using sharp tips at the anode of an ionisation chamber to increase locally the electric field. As in (5) the discrimination possible by the detection and measurement of both the direct light pulse and the recombination charge pulse will be discussed; however, the charge signal in eq. (16) is now 100 times the original ionisation charge. Similar resolutions were considered as, although the spread associated with charge multiplication may be larger than in the proportional scintillation case, the number of electrons collected is far greater than the number of photoelectrons so offsetting the first effect. Figure 10 shows the overlap in the light/charge ratios for equal numbers of incident alphas and betas for observed energies of 4 and 8 keV for an energy resolution of 40%.

The discrimination achievable using just the ratio alone is shown in fig. 11 by the circular points for a resolution of 40% and a $\ln(RS_{\text{signal}})$ cut of -7.3.

The discrimination is very similar to that for the proportional scintillation case, indeed the figure of merit values for 4 and 14 keV are 1.77 and 0.33. Again the reduced identification efficiency at low energies is due mainly to the loss of the primary light (less than 1% of events fail to give a charge pulse). Thus the efficiencies at low energies can be improved by classing events which produce only a charge pulse above a certain cut as beta induced and those giving S2 below as alpha induced. The improved

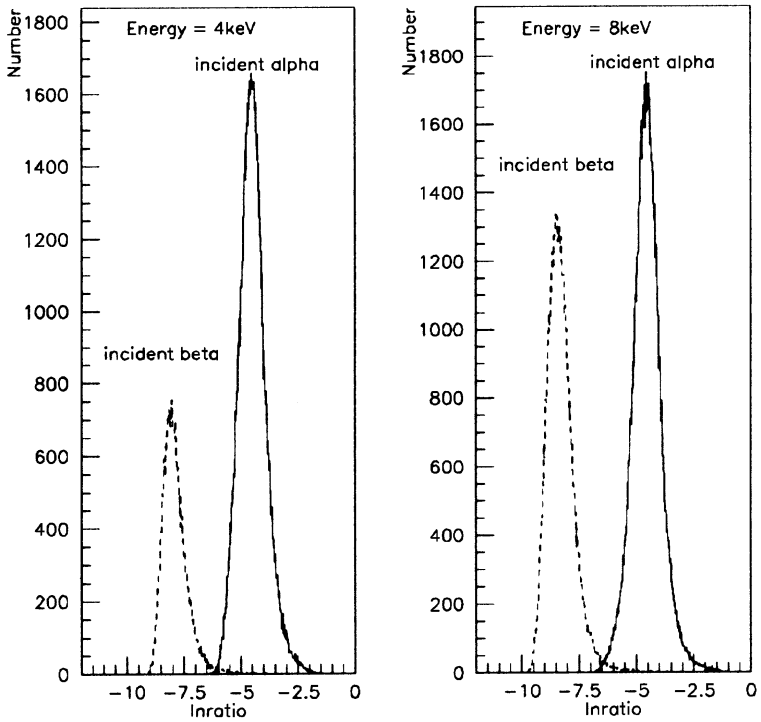

Fig. 10. – Overlap in light/charge ratios for alphas and betas with anode gain.

efficiency is shown by the square points; events which produce only an S1 pulse have been classed as alphas. The figure of merit values are again very similar to the proportional scintillation case. The likelihood technique could be applied to those events which produce only a primary light signal, as discussed in the previous section (the mean light signal sizes *vs.* energy are very similar for the anode tip case).

For both proportional scintillation and anode tips, as the efficiency of light collection is decreased the separation of alpha and beta events offered by the ratio remains the same but the number of events for which the primary light is unobserved increases. The proportional scintillation method is affected twice, for both S1 and S2. These losses increase rapidly with worsening resolution.

8. – Additional ideas

The collection efficiency of the energy seen as direct light (S1) may be increased by doping the LXe with TMA or the like. Such dopants are ionised by the photons emitted by the LXe and the greater efficiency of charge collection would increase the sensitivity of the experiment. Increases in charge collection of 30% for betas and more than a factor of 10 for alpha in comparison to undoped yields have been reported [30]. Thus it should be possible to detect signals of a few keV from both a beta and an alpha particle, *i.e.* the sensitivity of the experiment is improved as S1 is not detected directly, although the discrimination may well be worsened. For higher doping concentrations

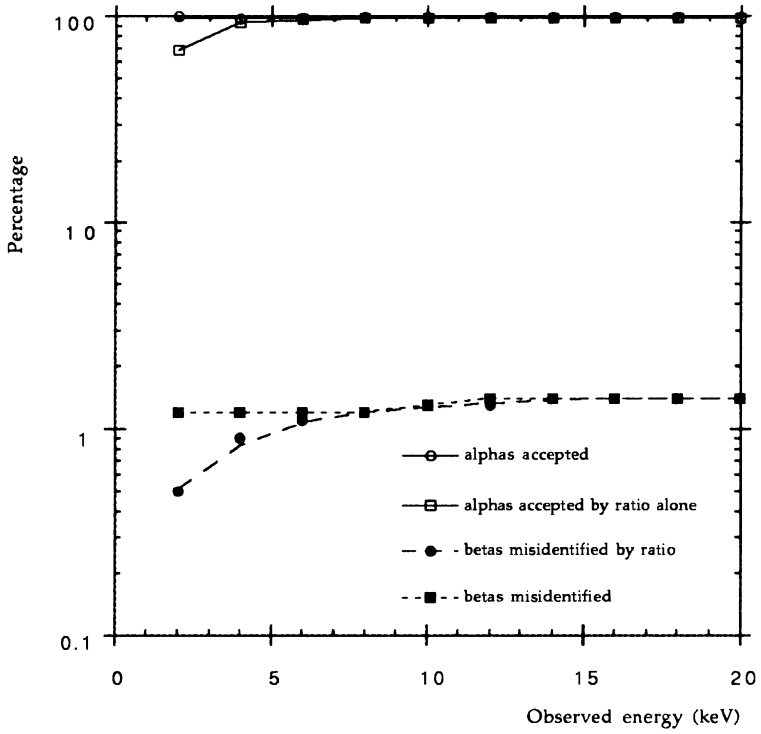

Fig. 11. – Percentage of events identified and misidentified.

all the UV light is absorbed and so discrimination is possible only via the time profile of the charge collection. Half the alpha light is emitted with a time constant of 3 ns, whilst three quarters of the beta light is associated with the delayed recombination process. The authors of [31] suggest that with low-noise electronics a timing resolution of 3 ns is possible with LXe. To view enough of the charge time profile for reasonable discrimination, amplification of the charge signal may well be necessary. Indeed electron multiplication was observed [30]. At an intermediate doping level applying a likelihood analysis to both the charge collection time profile and the light signal may prove advantageous.

The application of an electric field may also increase the light yield from heavily ionising particle as the electric field helps separate the ionisation charge, so limiting any possible quenching—recall that it has already been conjectured that quenching takes place in LXe for incident alpha. This increase has been seen in liquid argon for incident He ions [32]. Clearly, the applicability of this to dark matter searches is dependent upon the rather poorly known specific ionisation density of a recoiling nucleus/ion.

A particularly attractive technique for dark matter searches is the use of a Time Projection Chamber (TPC); this would give the direction in which the struck nucleus is recoiling and hence information on the direction of the incoming WIMP. Thus it is possible to take advantage of the 4 : 1 ratio in the number of forward to backward

recoils in the laboratory frame predicted for an isothermal, stationary DM halo [33]. Such a distribution of events is a unique signature for dark matter. The use of TPCs in the field of dark matter was originally proposed to search for cosmions using methane gas. Recent technological advances mean that TPCs should now be possible using both liquid and gaseous Xe; indeed several non-DM HEP experiments are proposed [34, 35]. The recoiling nucleus ionises the Xe gas, the electrons drift in the applied electric field and are then read out at the detector plane. The electron avalanche in the intense electric field close to the readout wires makes a TPC sensitive to small signals. A TPC may also only incorporate background rejection; however each requirement places tighter constraints on the maximum allowable pressure of the gas within it.

The great disadvantage of the TPC is its size. One needs approximately 0.5–1 cm of track to identify the direction of the incident particle and the nature of the recoiling particle. For a ~ 30 keV electron this corresponds to a gas pressure of about an atmosphere. Thus to achieve a target mass of ~ 1 kg, a detector volume of ~ 0.6 m^3 is required—this is not excessive. However, a recoiling nucleus travels a much shorter distance $\sim 10^{-6}$–$10^{-5}\,\mathrm{g\,cm^{-2}}$ for a recoil in the 3–30 keV range. Thus, pressures of 10^{-3}–10^{-2} of an atmosphere are required to see its track length. The resulting detector volume is ~ 600 m^3 (a big vacuum tank?). Whilst it would not be impossible to construct such a device, it is certainly very difficult and so only a long-term option. However, we suggest that a large gaseous TPC operated at a pressure at which electron tracks are identifiable yet a nuclear recoil is point-like, will have significant discrimination, very good sensitivity and sufficient mass—indeed such an option is currently under consideration [36]. Alternatively, the potentially excellent discrimination achievable with a device for which the nuclear recoil track is visible may allow significantly lower limits to be set from smaller mass detectors and is currently being investigated [37].

9. – Other noble liquids: LAr

Many of the ideas discussed so far are applicable to the other noble liquids, in particular to LAr. The use of a target with a lower atomic mass will offer increased sensitivity to lower-mass WIMPs and a reduced form factor. The same purification system may be used and, of particular interest as the need for scale-up due to the falling LSP cross-section becomes more important, LAr is considerably cheaper. Additionally, any radioactive ^{85}Kr may be easily removed as it is solid at LAr temperatures. Let us outline the discrimination achievable either by collecting the light alone (subsect. **9**˙1) or both light and charge (subsect. **9**˙2).

9˙1. *Collection of light alone: likelihood technique.* – LAr has a light yield comparable to LXe but at 130 nm [38]. The latter necessitates the use of a wavelength shifter as, although there are reflective coatings and transmitting window materials, the quantum efficiency of photocathodes for PMTs and the transmittance of the surface silicon dioxide of diodes is very small. POPOP has been used successfully [13] and one would expect the response of TPH to be better (or combination). As with LXe the light emission occurs from the singlet and triplet states. However, the recombination time for a minimum ionising particle is now 0.8 ns [8] and thus the light has the time constants of the excited states themselves. These are $t_1 \sim 6$ ns for the singlet and $t_2 \sim 1100$ ns for the triplet [13]. There are variations in the literature as to the exact size

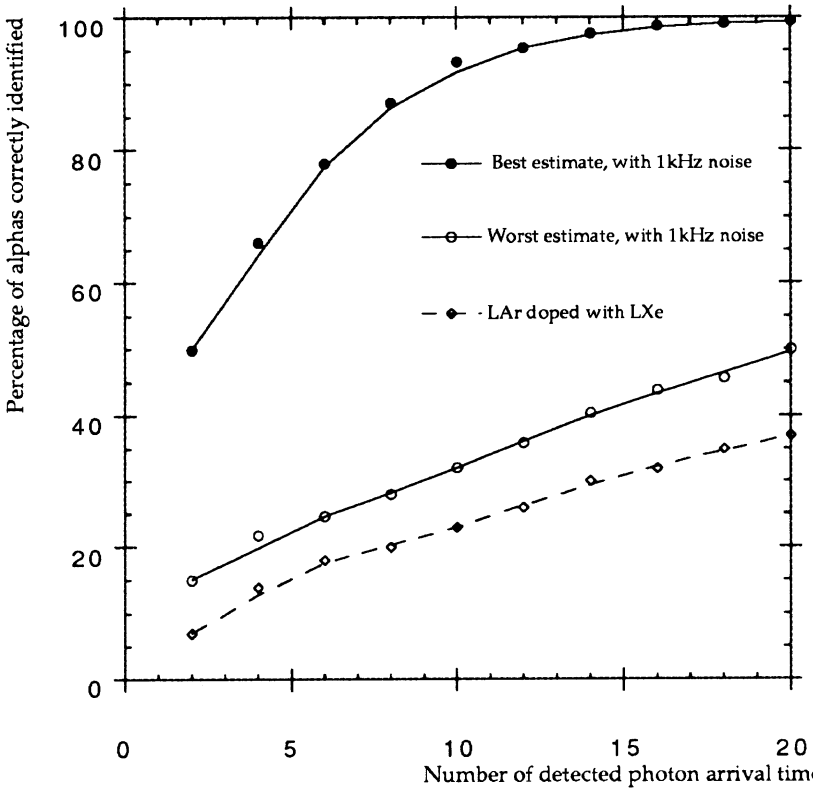

Fig. 12. – Percentage of alpha events identified correctly for 95% background rejection in LAr.

of the ratio A_1/A_2 for both betas and alphas, but all authors agree that there is a clear difference between them [13, 15, 16]. Although the lack of a long recombination time in the case of betas decreases the discrimination obtained, it is still nevertheless significant. Figure 12 shows the fraction of alphas correctly identified with a background rejection of 95%—the PMT single photoelectron pulse shape and random noise were included.

The variation arises from the spread in the measurements of A_1 and A_2. At best the discrimination is not significantly worse than the LXe case, but it must be remembered that the above numbers of photoelectrons will, in practice, correspond to a greater energy deposition than in the LXe case due to the inefficiency of the wavelength shifter (WLS) (an overall efficiency of $\leqslant 0.75$ is to be expected for a WLS coating [39]). The figure of merit values for 6 and 20 photon arrival times are 1.1–0.3 and 0.3–0.2.

An alternative to a conventional wavelength shifter is doping with LXe. The Xe converts the 130 nm light from the LAr to its emission wavelength of 175 nm [40, 41]. In fact an increase in light yield in comparison to pure LAr and POPOP has been observed using this technique [41]. Although the data is at present somewhat limited, there are differences in pulse shape between incident alpha and beta. Using the information contained in [40] the dashed curve in fig. 12 was obtained for a background rejection level of 95%. Whilst the discrimination is considerably less than for the pure

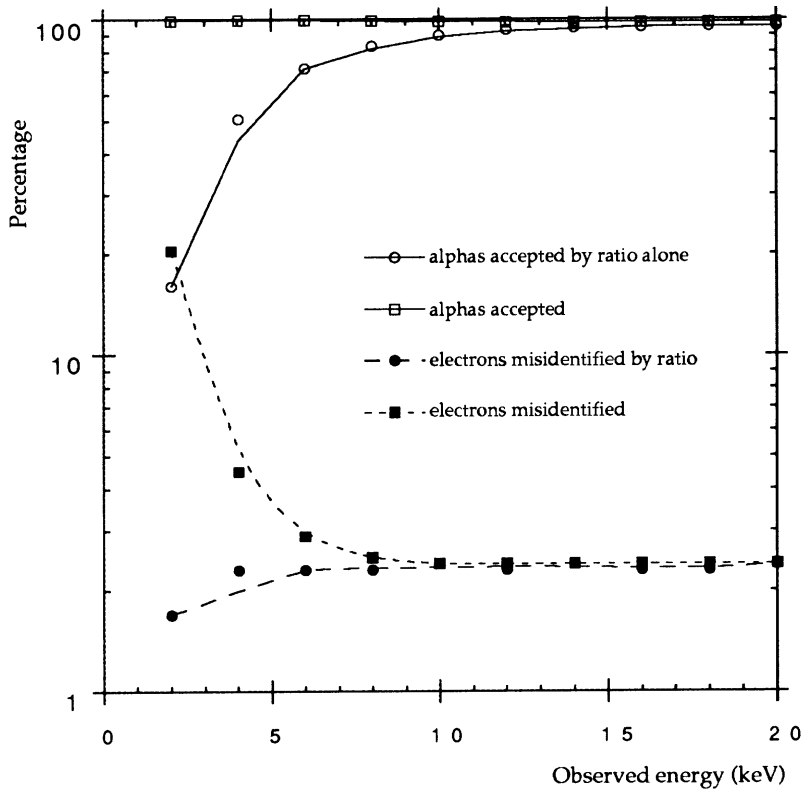

Fig. 13. – Discrimination obtained with proportional scintillation in LAr.

liquids, it is nevertheless an interesting option worthy of pursuit. The figure of merit values for 6 and 20 photon arrival times are 1.7 and 0.7. Let us now consider the application of an electric field.

9·2. *Recombination light/charge in* LAr. – The faster recombination time implies that one is less able to prevent the recombination light from forming; 23.6 eV is required to form an e^-/ion pair in LAr compared with 15.6 eV in LXe [42]. When an electric field is applied, the light yield is reduced by 65% [8]. For an incident alpha only 10% of the charge created is collected [30], whilst for an electron the collection efficiency is in excess of 90%. Thus there is a significant difference and discrimination is possible. Proportional scintillation and anode tips are considered in turn.

9·3. *Proportional scintillation in* LAr. – As in sect. **6**, the measurement of S1 and S2 along with the detection of the charge pulse associated with S2 are required. Using the same resolution, multiplication factor, light collection and threshold as in the LXe case, the discrimination obtained is shown by the circles in fig. 13 for the case where only those events that give both an S1 and S2 pulse are considered.

The worsened discrimination for betas is again caused by the fact that they are more likely to fail to give a direct light, S1, signal. The figure of merit values for 4 and 14 keV can be improved from 1.17 and 0.26 to 0.22 and 0.16 by again identifying single

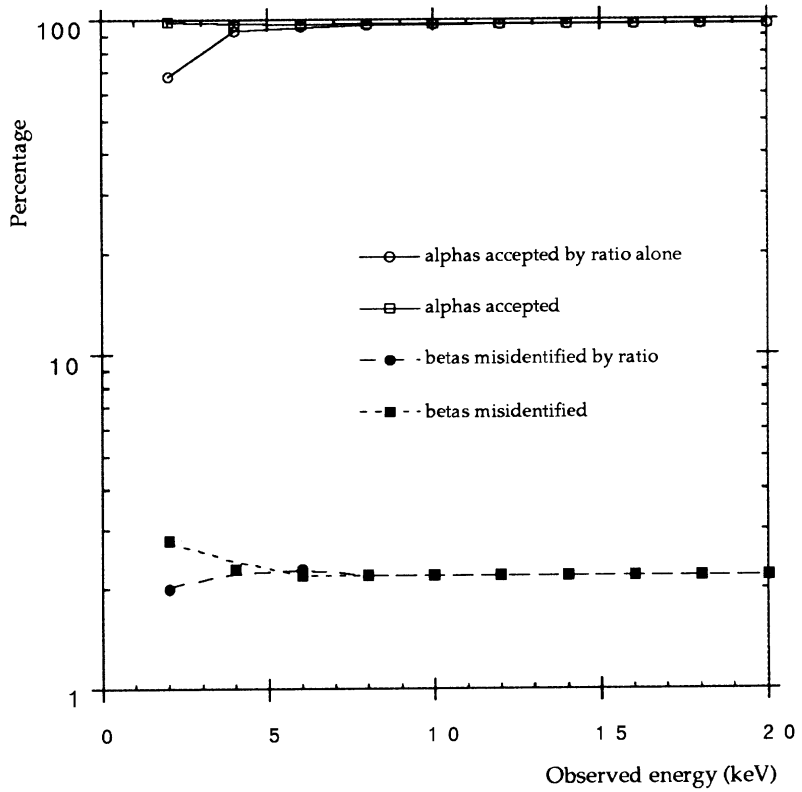

Fig. 14. – Discrimination obtained with anode tips in LAr.

pulses as S2 through the associated charge pulse; "S2 only" pulses below a given cut are classed as alpha induced and those above as beta induced. The improved discrimination is indicated by the squares in fig. 13.

The discrimination is slightly worse than for LXe, as one would expect from the decreased difference between alpha and beta charge collections.

Likewise it is possible to record the arrival times of the prompt photons and perform a likelihood ratio test on these in those cases where only S1 is seen.

9˙4. *Use of anode tips in* LAr. – Figure 14 shows the discrimination achieved with the same criteria as for LXe, both for the case where only those events producing both a light and charge pulse are considered (circles) and for the application of a cut on the charge signal for those events which fail to give a visible light pulse (squares).

The figure of merit values for 4 and 14 keV are 1.14 and 0.25 by ratio alone and 0.17 and 0.15 with the application of a cut. These values are slightly better than the LAr proportional scintillation case due to the greater amplification afforded with anode tips rather than proportional scintillation. However, it must be remembered that the spread associated with this higher gain will be larger.

10. – Conclusion

It would appear that very significant discrimination between nuclear recoil events and background beta/gamma events is possible at low energies using the noble liquids, in particular with LXe. This discrimination can be achieved both by the collection of the light alone with a likelihood analysis on the photoelectron arrival times and by the operation of dual light and charge measurements. The latter may either be performed in the proportional scintillation mode or via direct amplification of the charge signal (significant discrimination is possible even when only the charge signal is above threshold). The level of discrimination suggested by these Monte Carlo studies far exceeds that achievable with other scintillating targets such as sodium iodide where figures of merit in the range 1–5 have been achieved. Hence the extra time and money required to bring noble liquid targets to fruition is warranted as they offer one of the principal routes to the low events rates suggested for SUSY candidates.

* * *

We would like to thank those people within and outside the Dark Matter Collaboration who have helped with this work and the preparation of this manuscript. The author would like to acknowledge the support of the PPARC under the post-doctoral fellowship scheme.

REFERENCES

[1] ELLIS J. and FLORES R. A., *Nucl. Phys. B*, **307** (1988) 883; GRIEST K., *Calculations of rates for direct detection of neutralino dark matter*, FERMILAB-Pub-88/52-A (1988); ELLIS J. and FLORES R. A., *Phys. Lett. B*, **263** (1991) 259; BOTTINO A. *et al.*, *Search for neutralino dark matter with* NaI *detectors*, LNGS 92/7; BARBIERI R. *et al.*, *Nucl. Phys. B*, **313** (1989) 725; ELLIS J. and FLORES R. A., CERN-TH-6483/92, CERN, Geneva (1992).
[2] SMITH P. F., Review talk, *Proceedings of the I International Symposium on Sources of Dark Matter in the Universe*, edited by D. CLINE (World Scientific) 1995; BACCI C. *et al.*, *Phys. Lett. B*, **293** (1992) 330; GERBIER G., *Proceedings of the XXVI Rencontre de Moriond* (Editions Frontières, Gif-sur-Yvette) 1991, p. 470.
[3] DAVIES G. J. *et al.*, *Phys. Lett. B*, **320** (1994) 395; SPOONER N. J. C. and SMITH P. F., *Phys. Lett. B*, **314** (1993) 430.
[4] APRILE E. *et al.*, *Nucl. Instrum. Methods A*, **302** (1991) 177.
[5] BRAEM A.. *et al.*, *Nucl. Instrum. Methods A*, **320** (1992) 228.
[6] YPSILANTIS T. *et al.*, *Nucl. Instrum. Methods A*, **323** (1992) 583.
[7] APRILE E. *et al.*, *IEEE*, **37** (1990) 533.
[8] KUBOTA S. *et al.*, *Phys. Rev. B*, **17** (1978) 2762; **20** (1979) 3486.
[9] KUBOTA S. *et al.*, *J. Chem. Phys.*, **11** (1978) 2645.
[10] MASUDA K., *Liquid xenon calorimeters*, talk given at *The Conference on Very High Resolution Electromagnetic Calorimetry, Sitguna, Sweden, November 9-11, 1989*.
[11] MARTIN M., *J. Chem. Phys.*, **50** (1971) 3289.
[12] DRUGER S. *et al.*, *J. Chem. Phys.*, **50** (1969) 3143.
[13] KUBOTA S. *et al.*, *Nucl. Instrum. Methods*, **196** (1982) 101.
[14] KUBOTA S. *et al.*, *Phys. Rev. B*, **21** (1980) 2632.
[15] HITACHI A. *et al.*, *Phys. Rev. B*, **27** (1983) 5279.
[16] JORTNER J. *et al.*, *J. Chem. Phys.*, **42** (1965) 4250; SUEMENTO T. *et al.*, *J. Phys. Soc. Jpn.*, **46** (1979) 1554; CARVALHO M. J. *et al.*, *J. Lumin.*, **18/19** (1979) 487.

[17] BIRKS J. B., *Theory and Practice of Scintillation Counting* (Pergamon Press Ltd.) 1964.
[18] HITACHI A. *et al.*, *Nucl. Instrum. Methods*, **196** (1982) 97; HITACHI A. *et al.*, *Phys. Rev. B*, **23** (1981) 4779; MUTERER M., *Nucl. Instrum. Methods*, **196** (1982) 77.
[19] MASUDA K. *et al.*, *Nucl. Instrum. Methods*, **160** (1979) 247; MASUDA K. *et al.*, *Nucl. Instrum. Methods*, **174** (1980) 439.
[20] ICHINOSE H. *et al.*, *Nucl. Instrum. Methods A*, **305** (1991) 111; MULLER R. A., *Phys. Rev. Lett.*, **27** (1971) 532.
[21] SUZUKI S. *et al.*, *Nucl. Instrum. Methods A*, **245** (1986) 78.
[22] ASTRONOMY/PARTICLE PHYSICS JOINT PROJECT, *Galactic Dark Matter Search*, status and first results (1993-94) and proposed future programme (1995-99).
[23] DAVIES G. J., *Development of a liquid xenon detector for use in dark matter searches*, PhD Thesis, University of London (1994).
[24] BROOKS F. *et al.*, *Nucl. Phys. A*, **465** (1987) 429.
[25] BELLI P. *et al.*, *Nucl. Instrum. Methods A*, **336** (1993) 336.
[26] BENETTI P. *et al.*, *Nucl. Instrum. Methods A*, **327** (1993) 203.
[27] ZEPLIN detector, informal RAL/ICSTM/UCLA HEP collaboration.
[28] PARK J., *Liquid xenon: WIMPs detector using wave-shifting fibres*, talk given at *Critique of the Source of Dark Matter in the Universe, UCLA, February 1994*, *Proceedings of the 1st International Symposium on Sources of Dark Matter in the Universe*, 1994, p. 288.
[29] BRESSI G. *et al.*, *Nucl. Instrum. Methods A*, **310** (1991) 613.
[30] HASEGAWA Y. *et al.*, *Nucl. Instrum. Methods A*, **327** (1993) 57.
[31] LEBEDEV P. K. and MURAVIEV S. V., *Nucl. Instrum. Methods A*, **327** (1993) 138.
[32] HITACHI A. *et al.*, *Phys. Rev. B*, **46** (1992) 540.
[33] SPERGEL D. N., *Phys. Rev. D*, **37** (1988) 1353.
[34] CARUGNO G. *et al.*, *Nucl. Instrum. Methods A*, **311** (1992) 628.
[35] LAURENTI G. *et al.*, *A study of a high rate solar neutrino detector with neutrino energy determination*, CERN/LAA/93-10.
[36] YPSILANTIS T., private communication.
[37] BUCKLAND K. N. *et al.*, *Phys. Rev. Lett.*, **73** (1994) 1067.
[38] DOKE T. *et al.*, *Nucl. Instrum. Methods A*, **290** (1990) 617.
[39] HITACHI A. *et al.*, *Nucl. Instrum. Methods*, **196** (1982) 97.
[40] BLOUKE M. M. *et al.*, *Appl. Optics*, **19** (1980) 3318.
[41] KUBOTA S. *et al.*, *Nucl. Instrum. Methods A*, **327** (1993) 71.
[42] SUZUKI M. *et al.*, *Nucl. Instrum. Methods A*, **327** (1993) 67.